Langmuir

Article

pubs.acs.org/Langmuir

Self-assembly of Class II Hydrophobins on Polar Surfaces

Mathias S. Grunér,[†] Géza R. Szilvay,[†] Mattias Berglin,[‡] Michael Lienemann,[†] Päivi Laaksonen,[†] and Markus B. Linder*[,†]

[†]VTT Technical Research Centre of Finland, Biotechnology, Tietotie 2, FIN-02044 VTT, Espoo, Finland

[‡]Department of Cell and Molecular Biology, Interface Biophysics, Göteborg University, SE-40530 Göteborg, Sweden

ABSTRACT: Hydrophobins are structural proteins produced by filamentous fungi that are amphiphilic and function through self-assembling into structures such as membranes. They have diverse roles in the growth and development of fungi, for example in adhesion to substrates, for reducing surface tension to allow aerial growth, in forming protective coatings on spores and other structures. Hydrophobin membranes at the air−water interface and on hydrophobic solids are well studied, but understanding how hydrophobins can bind to a polar surface to make it more hydrophobic has remained unresolved. Here we have studied different class II hydrophobins for their ability to bind to polar surfaces that were immersed in buffer solution. We show here that the binding under some conditions results in a significant increase of water contact angle (WCA) on some surfaces. The highest contact angles were obtained on cationic surfaces where the hydrophobin HFBI has an average WCA of 62.6° at pH 9.0, HFBII an average of 69.0° at pH 8.0, and HFBIII had an average WCA of 61.9° at pH 8.0. The binding of the hydrophobins to the positively charged surface was shown to depend on both pH and ionic strength. The results are significant for understanding the mechanism for formation of structures such as the surface of mycelia or fungal spore coatings as well as for possible technical applications.

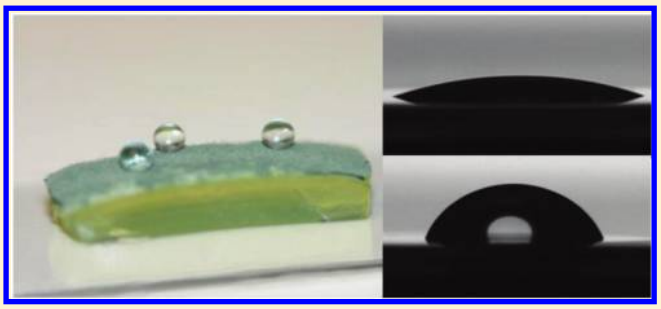

1. INTRODUCTION

Hydrophobins are structural proteins that fulfill many different tasks in the growth and development of filamentous fungi. They were first discovered as highly expressed genes and have subsequently been found in all filamentous fungi studied.[1] Sequence analysis suggested that hydrophobins could be divided into two classes, class I and class II.[2] Analysis of the properties of hydrophobins has shown that the division is useful since it reflects some clear functional differences. Both classes readily assemble into different types of supramolecular structures, most notably into membrane structures at interfaces. The clearest difference between the classes is that the structures formed by class I members are often very stable and can be disassembled only by using harsh conditions such as strong acids. In both classes the membranes seem to have multiple functions such as adhesion, formation of coatings on spores or fruiting bodies, and even to facilitate the formation of aerial structures.[3]

The determination of the three-dimensional structure of a class II hydrophobin, HFBII from *Trichoderma reesei*, suggested a mechanism for membrane formation.[4] HFBII has an almost globular structure that is highly cross-linked by disulfide bonds. One face of the protein shows nearly exclusively aliphatic hydrophobic residues. The rest of the protein shows typical hydrogen-bonding and charged residues which makes the molecule amphiphilic. Another class II hydrophobin HFBI showed an almost identical structure[5] whereas the class I EAS[6] hydrophobin protein had the same overall fold but did not have such a distinct amphiphilic structure. Furthermore, the EAS hydrophobin showed more loop-structures possibly reflecting the involvement of additional interactions on the route to self-assembly.

The amphiphilic structure explains the localization of hydrophobins to interfaces between polar and nonpolar substances such as the air−water interface and on hydrophobic surfaces in water.[7−12] There are also several observations indicating that molecular interactions between hydrophobin molecules in the plane of the interfacial layer play a significant role in stabilizing it. One such observation is the very high elasticity of membranes at the air−water interface,[12] and another observation is the highly organized two-dimensional crystalline structures observed at these interfaces.[13−15]

Self-assembly at interfaces is one of the most special properties demonstrated for hydrophobins. It is interesting that assembly occurs at different interfaces for apparently different reasons. The assembly at the air−water interface is related to the formation of aerial structures in moist or submerged conditions.[8] The assembly at hydrophobic interfaces can be related to adhesion of fungi to different substrates.[16] They also have the property to "recruit" other proteins to surfaces.[17] It has also been shown that hydrophobins are involved in making spores or other structures hydrophobic.[18,19] Both adhesion to hydrophobic surfaces[10,11,20−22] and assembly at the air−water interface[7,8,14,15,23,24] have been studied extensively, but mechanisms

Received: July 12, 2011
Published: February 9, 2012

for the assembly of hydrophobins on polar (hydrophilic) surfaces under aqueous conditions has not been well studied to date. However, understanding the mechanisms that allow hydrophobins to form hydrophobic coatings on hydrophilic surfaces is of great importance for understanding the interactions of fungi with their environment and the formation of hydrophobic hyphae[8,25] and spores.[18]

Observations of filamentous fungi show that the structures formed by their mycelia can be very hydrophobic (see Figure 1), and it is interesting to consider the role of hydrophobins in

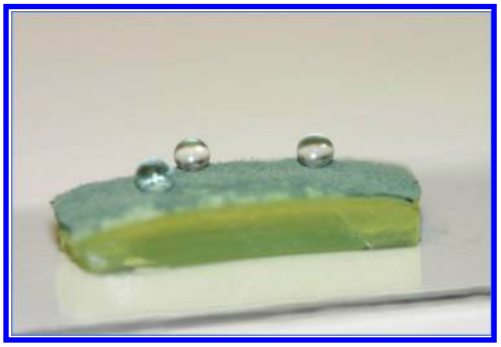

Figure 1. Surface of a mycelial mat of *T. reesei* growing on agar is highly hydrophobic as shown by water drop contact angles of about 140°.

forming this hydrophobicity.[25] This mechanism is important to understand when investigating the interactions of fungi with their environment, as demonstrated for example by the finding that hydrophobin coatings are critical for the infective pathways of fungi.[26] There may also be interesting applications for coating materials emerging from the understanding of such routes.

In this work, we were interested in how class II hydrophobins in aqueous solution could assemble on a solid polar hydrophilic surface so that the hydrophobic side of the membrane would face outward significantly reducing the polarity of the surface. It is already known quite well how hydrophobin layers are formed on hydrophobic surfaces.[27,28] The mass of such layers corresponds to a monomolecular layer of protein, suggesting that the hydrophobin binds with its hydrophobic patch to the hydrophobic surface and exposes its hydrophilic side out toward the hydrophilic surroundings. Interestingly, it was found that this hydrophilic side has some unexpected properties. It was found that other proteins could readily bind to the assembled hydrophobin layer from the water exposed side.[11] However, binding was highly dependent on pH and experiments showed that the hydrophilic side of the membrane exposes charges in such a way that efficient electrostatic interactions are formed with molecules in solution under suitable conditions. The binding properties of the hydrophobin layers are likely to be linked to the organized and repetitive structure of the hydrophobin layers. The biological role of this function is not known, but it suggests a way in which the hydrophilic side of the protein membrane could interact with other molecules or structures. One function could be to recruit other proteins to surfaces or to mediate anchoring of hydrophobins on spores or cell walls. This led us to investigate if a similar mechanistic study could show how membranes of class II hydrophobins could form on polar charged surfaces.

2. MATERIALS AND METHODS

Reagents and Chemicals. The class II hydrophobin proteins HFBI, HFBII, and HFBIII, were purified from *T. reesei* mycelium or culture supernatant using two-phase extraction and reversed phase chromatography as described earlier.[29,13]

The buffers used for protein adsorption experiments at different pHs were 10 mM sodium acetate (pH 4.0, 5.0), sodium phosphate (pH 6.0, 7.0), Tris-HCl (pH 8.0), and glycine−NaOH (pH 9.0, 9.5, 10.5). Hydrophobin adsorption was studied at a narrow pH range using buffers 10 mM Na−borate (pH 7.5−8.8) and glycine−NaOH (pH 8.6−9.9). For ionic strength experiments, the following buffers were used: 10 mM Na−borate at pH 8.9 with 10−500 mM NaCl.

Preparation of SAM Layers. Self-assembled monolayers (SAMs)[30] were prepared to form cationic, anionic, and nonpolar aliphatic surfaces. For preparing cationic surfaces *N,N,N*-trimethyl-(11-mercaptoundecyl)ammonium chloride ($HS(CH_2)_{11}NMe_3^+Cl^-$) thiol (TMA) (pK_a 9.76[31]) (Prochimia Surfaces, Poland) was used, for hydrophobic surfaces 1-hexanethiol (HEX) (Sigma-Aldrich, USA) was used, and for anionic surfaces 1-mercaptoundecanoic acid (MUA) (pK_a 4.80[32]) (Sigma-Aldrich) was used.

The SAM coatings were prepared either on gold coated quartz crystal microbalance with dissipation monitoring (QCM-D) sensor disks (QCX 301, Q-Sense AB, Sweden) or on gold coated glass disks (with a chromium adhesion layer) (Bionavis, Finland). The procedure for coating was as follows: The substrates were cleaned in a UV/ozone chamber (Procleaner, Bioforce) for 10 min followed by a 10 min heating in a mixture of $H_2O/NH_3/H_2O_2$ (5:1:1) at 75 °C. Disks where then cleaned thoroughly with Milli-Q (Millipore) followed by a second UV/ozone cleaning. The discs where then immersed overnight at ambient temperature (21 °C) in 10 mM SAM reagents dissolved in ethanol. Before use, the substrates were rinsed with ethanol and Milli-Q water and dried with N_2 (g).

Preparation of Cationic Polymer Surfaces. For forming cationic polymer surfaces, the polymer polyethylenimine (PEI) (Sigma-Aldrich) was spin coated on SiO_2 QCM-D sensor discs (QSX 303, Q-Sense AB, Sweden). A 40 μL drop of 1 g/L PEI in Milli-Q was spin coated on the SiO_2 discs in atmospheric pressure for 90 s at 3000 rpm and dried.

Hydrophobin Adsorption Measured Using QCM-D. QCM-D was used to measure resonance frequency and dissipation simultaneously and to thereby calculate the mass of the bound protein layer (D4-QCM system, Q-Sense AB, Sweden). The adsorbed mass per areal unit was calculated from the resonance frequency changes using the Sauerbrey relation, $\Delta m = -C\Delta f/n$, where Δm is adsorbed mass, Δf is frequency change, C = 17.7 ng·Hz·cm^{-2}, and using the third overtone (n = 3). By combining the frequency measurements with dissipation measurements, it becomes possible to determine whether the bound protein layer is rigid or soft (water rich).[33] The dissipation value (D) is a measure of how rapidly the oscillations decay, describing the viscoelastic properties of the protein layer. A rigid material results in low dissipation values, whereas a softer renders higher values.

Hydrophobins (HFBI, HFBII, and HFBIII) were dissolved in buffer at 0.1 mg/mL. Protein solution (300 μL) was pumped through the measuring chamber with a flow rate of 100 μL/min. The sensors were left to stabilize after adsorption for 30−80 min until a stable signal was achieved and were then washed with the running buffer.

Hydrophobin Adsorption onto Submerged Substrates. Hydrophobin protein HFBI was diluted to 0.1 mg/mL in different buffer solutions with varying pH. SAM coated glass disks (Bionavis), described above, were immersed in the protein solution for about 45 min. The disks were then washed with buffer and left to soak in an excess of buffer for 10 min. The disks were then washed thoroughly in Milli-Q water before being dried with N_2 (g).

Water Contact Angle Measurements. For water contact angle (WCA) measurements, an optical contact angle and surface tension meter (CAM 200, KSV NIMA, Finland) was used. A 6 μL drop of Milli-Q water was applied on the surface under study and the average contact angle was calculated from a series of 15 pictures taken with a 5 s interval. The WCA was measured before and after each protein

adsorption experiment. The reported WCA values were determined as the average of three measurements.

Surface Characterization by Impedance Measurements. Impedance measurements were made using a z-LAB instrument (Layerlab AB, Sweden). This device is based on resonance enhanced surface impedance technology (RESI) and is here used to monitor changes in impedance in order to distinguish between loose and dense layers as well as the insulating properties of a protein layer. An increase in capacitance value indicates the formation of a less insulating layer.[34] Gold coated surfaces (ZO-PADS, Layerlab) were used in all experiments. The sensors were coated with SAMs as described above. For SAM coating, the sensors were first cleaned in a $H_2O/NH_3/H_2O_2$ mixture (5:1:1) at 75 °C for 10 min. The discs were then immersed overnight at room temperature in SAM reagent as described above. Before experiments, the sensors were sonicated in pure ethanol, cleaned with Milli-Q water, and dried with N_2 (g). Measurements were done using HFBI (0.1 mg/mL) in 50 mM glycine−NaOH at pH 8.9. The sample was injected (75 μL at a flow rate 25 μL/min for 3 min), and the sensor was allowed to stabilize for 10−30 min until a stable baseline was obtained. The sensors were then washed with buffer at 25 μL/min. All measurements were done in triplicate. The capacitance of the protein layer, $C_{Protein}$, was calculated from the SAM capacitance, C_{SAM} which is measured just before protein injection, and the total capacitance, C_{Total}, which is measured after wash, using the formula: $C_{Protein} = 1/((1/C_{Total}) - (1/C_{SAM}))$.

Atomic Force Microscopy (AFM). For AFM imaging protein layers were prepared on flame annealed gold chips (Arrandee, Germany) coated with HEX or TMA SAMs as described above for hydrophobin adsorption onto submerged substrates. After protein adsorption and washing, the samples were immediately imaged in water without drying in between. Imaging was done in water using a NanoScope IIIa Multimode AFM ("E" scanner; Digital Instruments/Bruker) as described earlier[14] using silicon nitride cantilevers (NP-S, Veeco) with a force constant of 0.32 N m^{-1}. Roughness analysis was performed using the software Scanning Probe Image Processor, SPIP (Image Metrology, Denmark).

3. RESULTS

Adsorption of Hydrophobins to Surfaces. Hydrophobin adsorption to hydrophobic, cationic, and anionic surfaces was investigated using QCM-D. Figure 2 shows representative adsorption curves of HFBI binding on SAM surfaces of TMA (cationic) at pH 9.5, HEX (hydrophobic) at pH 9.0, and MUA (anionic) at pH 9.0. The WCA was measured on all QCM-D sensor chips before and after the QCM-D adsorption experiments. After protein adsorption had reached a maximum, the surfaces were rinsed with buffer to remove any loosely bound protein. Control experiments were made by identical treatments of the surfaces but leaving out the protein.

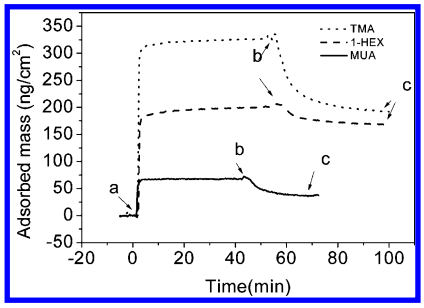

Figure 2. QCM-D sensograms showing representative curves of HFBI binding to different SAM surfaces. The surfaces used were hydrophobic HEX (at pH 9.5), anionic MUA (at pH 9.0), and cationic TMA (at pH 9.0). Part a corresponds to hydrophobin injection, part b to buffer wash, and part c to end of buffer wash where adsorbed mass and WCA was measured. The adsorbed mass was calculated from resonance frequency change between the initial point (a) and the final point (c).

Hydrophobic Surfaces. The mass of HFBI and HFBII adsorption on hydrophobic HEX SAM was observed by QCM-D (Figure 3). The measured values of adsorbed mass on the HEX SAM surface were between 170 and 282 ng/cm^2 depending on pH (Figure 3A). The adsorption reached maximum levels within minutes and washing with buffer typically removed only about 10% of adsorbed protein. Dissipation changes were typically below 0.2 in all experiments indicating a rigid layer. The WCA was measured for all QCM-D sensor chips before and after the QCM-D adsorption experiments. The WCA of the freshly prepared HEX SAM was 92.0 ± 6.3° before deposition. After protein adsorption, the surfaces were clearly more hydrophilic with WCA values between 39° and 56°, and between 38° and 50°, for HFBI and HFBII, respectively (Figure 3B). To confirm results, we also tested the possible effect of having longer chain SAMs by using undecanethiol SAM surfaces. On the undecanethiol surface, the mass of bound HFBI was 262 ng/cm^2 and resulting WCA 34.9 ± 3° at pH 9 showing that chain length did not affect binding.

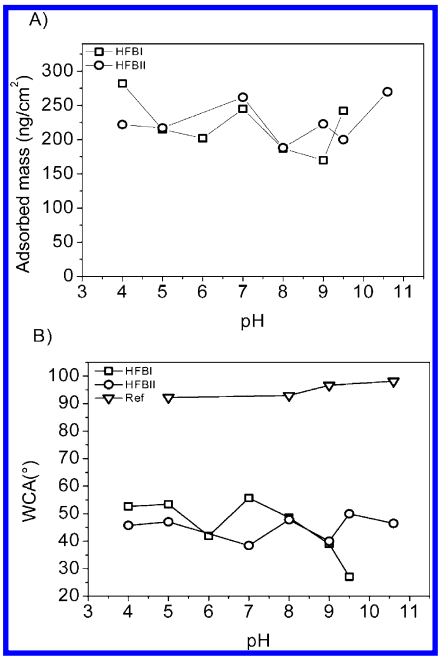

Figure 3. Adsorption of hydrophobins on hydrophobic surfaces. (A) Graph of adsorbed mass of HFBI and HFBII on hydrophobic HEX SAM as a function of pH as observed by QCM-D. (B) WCAs as a function of pH of the HEX SAM coated QCM-D sensors after HFBI or HFBII adsorption. A negative control surface (labeled ref) was treated similarly but without addition of protein. The standard deviation for HFBI on HEX SAM was ±6.7° (N = 3) at pH 9.

Cationic Surfaces. The binding of HFBI, HFBII, and HFBIII was studied on two types of cationic surfaces; TMA SAM and spin coated polymer PEI. The protein adsorption to the TMA SAM surface was measured using QCM-D over a pH range between 4.0 and 10.5 (Figure 4A). The corresponding WCAs were measured on QCM-D sensors before and after protein adsorption, and are shown in Figure 4B. Before deposition, the TMA SAM had a WCA of about 22.3° (±5.7°). For hydrophobin adsorbing on a TMA SAM, close to half of the initially bound mass was typically removed from the surface during the wash step (Figure 2). The dissipation changes were

dx.doi.org/10.1021/la300501u | Langmuir 2012, 28, 4293−4300

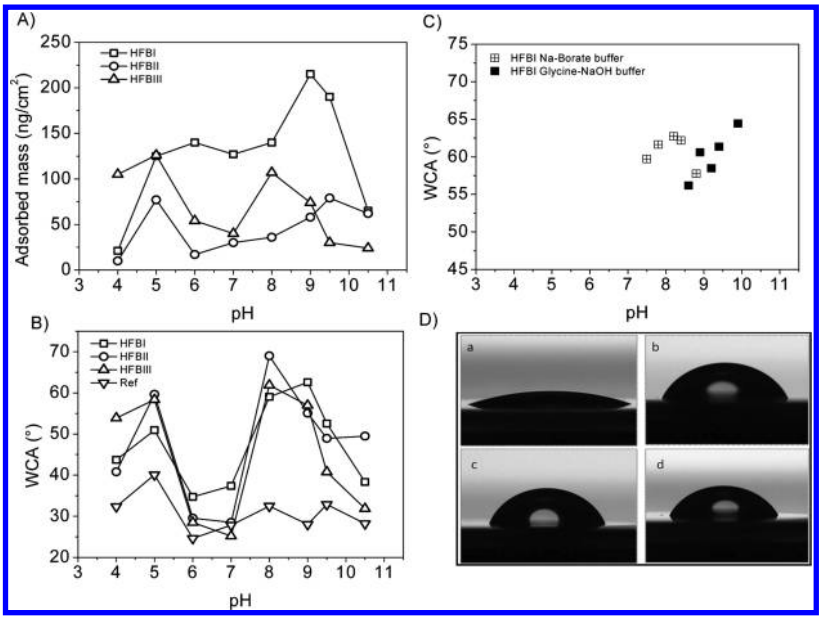

Figure 4. Adsorption of hydrophobins on cationic SAM surfaces. (A) QCM-D derived adsorbed mass of HFBI, HFBII, and HFBIII on TMA SAM surface as a function of pH. (B) WCAs of the same surfaces after hydrophobin adsorption in QCM-D runs as a function of pH. WCAs after HFBI, HFBII, or HFBIII adsorption are shown, as well as a negative control surface (labeled ref) that was treated similarly but without addition of protein. (C) WCA of HFBI on a TMA SAM surface at a narrow pH range. (D) Water drop profile shapes from WCA measurements on TMA SAM surfaces before protein coating (a), after HFBI (at pH 9.0) (b), HFBII (at pH 8.0) (c), and HFBIII (at pH 8.0) (d) coating. The obtained WCAs were 22.3° before deposition, and 62.6°, 69.0°, and 61.9°, after HFBI, HFBII, and HFBIII adsorption, respectively.

below 0.2 in all experiments indicating that all the layers formed had a rigid structure. For HFBI, the maximum of adsorbed mass (215 ng/cm^2) was obtained at pH 9.0. The value is close to what is expected for a monolayer based on an approximate calculation using the dimensions of the protein (2.2 nm × 2.2 nm) which gives a weight for a monolayer of about 250 ng/cm^2.[5]

WCA as a function of pH for HFBI, HFBII, and HFBIII as well as a buffer control on TMA are shown in Figure 4B. All three proteins show a similar dependency of WCA on pH with a smaller peak at pH 4.0−5.0 and a maximum WCA peak at pH 8.0−9.0. The smaller WCA peak at pH 4.0−5.0 had a very similar shape for all three hydrophobins and the negative control. However, at the maximum peak around pH 8.0−9.0, the WCAs of hydrophobin samples are clearly higher (60−70°) than the buffer only sample (28−30°). HFBI has a maximum value of WCA of 62.6° at pH 9.0, HFBII, a maximum of 69.0° at pH 8.0, and HFBIII, a maximum of 61.9° at pH 8.0. The influence of the type of buffer used was examined by changing the 10 mM phosphate buffer for experiments at pH 6 and 7 for HFBI and HFBII on TMA SAM to Na-citrate (10 mM, pH 6) or Tris-HCl (10 mM, pH 7). The WCA values showed moderate changes with WCA values for HFBI increasing from 34.7° to 39.1° at pH 6 and 37.4° to 44.3° at pH 7. For HFBII, the values were changed from 29.5° to 32.2° at pH 6 and 28.5° to 38.8° at pH 7.

To confirm results and study the effect of the type of buffer used we investigated the binding to TMA SAM at a selected narrow pH range in more detail (Figure 4C). A pH range of 7.5−9.9 was probed using 10 mM Na−borate (pH 7.5−8.8) and glycine−NaOH (pH 8.6−9.9) buffers in room temperature. Using the Na−borate buffer, the WCA has a maximum at pH 8.2 with a 62.7° WCA. There are variations between the two used buffers as seen in the samples with overlapping pHs. Some of this variation (roughly 5°) could be due to experimental variation, but a small buffer related effect is likely to exist.

Water drop profiles at pHs on cationic surfaces with the highest average WCA for each protein are shown in Figure 4D. The cationic surface without protein shows a low contact angle (Figure 4D, a), but after hydrophobin treatment, the WCA markedly increases (Figure 4D, b−d for HFBI, HFBII, and HFBIII, respectively).

Cationic PEI Surfaces. To study the effect of the underlying charged surface on the assembly of hydrophobin the adsorption, QCM-D, and WCA experiments were repeated using a cationic polymer (PEI) instead of the cationic TMA SAM as the underlying layer. The amount of adsorbed HFBI mass on PEI as a function of pH and the corresponding WCAs are shown in Figure 5. The spin-coated PEI surface had a WCA below 10° before deposition. The amount of adsorbed HFBI as a function of pH shows a peak at pH 5 where 150 ng/cm^2 is adsorbed and an increased binding at basic pHs with a maximum value of 260 ng/cm^2 adsorbed protein at pH 10. The pH dependency of HFBI binding to PEI was very similar to the binding to TMA. The adsorption of HFBI on the PEI surface generates two peaks of WCA as a function of pH. The resulting WCA values as a function of pH (Figure 5B) show two peaks: the smaller peak measured at pH 5.0 with a 30.3° WCA and a second, maximum peak at pH 8 with a WCA of 50.3°.

Adsorption on Anionic Surfaces. The effect of surface charge was studied by using an anionic and highly hydrophilic MUA SAM and following the binding of HFBI as well as a negative control without protein (buffer only) to this surface (Figure 6). Before protein deposition, the MUA SAM had a WCA of about 31.5° (±3.3°). At low pH, there was significant protein binding with amounts close to a monolayer, but the binding rapidly decreased with increasing pH. For both HFBI and the buffer control, the WCAs were lower than before adsorption on the MUA SAM over the whole pH range. The

dx.doi.org/10.1021/la300501u | Langmuir 2012, 28, 4293−4300

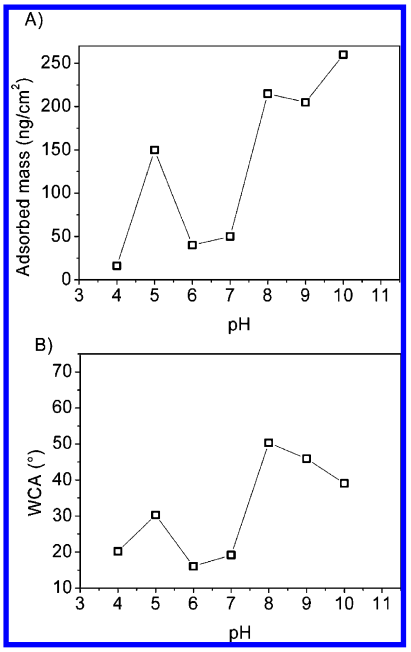

Figure 5. Adsorption of HFBI on cationic PEI surfaces. (A) Mass of adsorbed HFBI on cationic PEI surface as observed by QCM-D at various pHs. (B) WCAs of HFBI coatings on PEI after QCM-D measurements as a function of pH. The WCA of PEI surface before deposition was <10°.

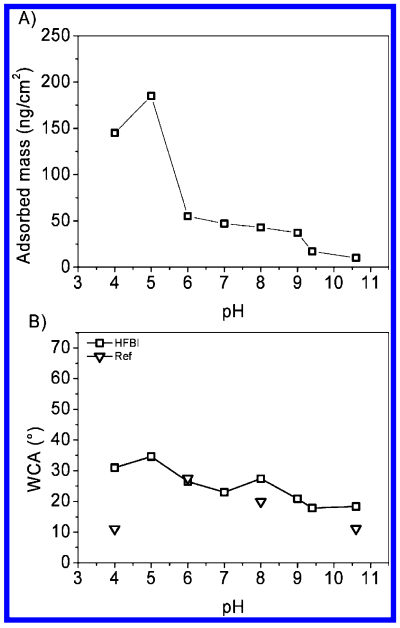

Figure 6. Adsorption of HFBI on anionic MUA SAM. (A) QCM-D derived mass of adsorbed HFBI on MUA as a function of pH. (B) WCAs of the same surface after HFBI adsorption as well as a negative control surface (labeled ref) that was treated similarly but without addition of protein are shown.

results show that HFBI interactions with anionic surfaces were very different from interactions with cationic surfaces.

Effect of Ionic Strength. The nature of the interaction between the cationic TMA SAM and HFBI was studied by following binding and WCA with increasing ionic strength. A 10 mM glycine buffer at pH 9.0 with NaCl at different concentrations (0, 10, 25, 50, 75, 100, 500 mM) was used. The results show that both bound mass and WCA rapidly decrease with increasing ionic strength, which indicates a role for ionic interactions in the layer formation (Figure 7). However, HFBI

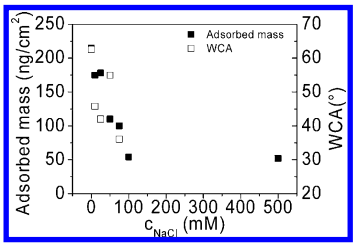

Figure 7. HFBI adsorption to cationic TMA SAMs as a function of NaCl concentration. QCM-D derived adsorbed mass and WCA are shown. The protein adsorption was done at pH 9.0.

adsorption to the cationic surface could not be completely inhibited even at 500 mM NaCl, and it is possible that at such high ionic strengths the hydrophobic interactions between the SAM and HFBI are promoted.

Characterization by Capacitance. The capacitance of the HFBI layer was measured for both cationic TMA and hydrophobic HEX SAMs at pH 8.9. The capacitance of HFBI on the HEX SAM surface was 5.0 ± 0.8 μF/cm^2 while the capacitance of HFBI on the cationic TMA SAM was 73.7 ± 29.3 μF/cm^2. The much lower capacitance value on the hydrophobic surface compared to the cationic surface indicates that the binding of HFBI on the hydrophobic surface is denser and results in an insulating layer, while the binding to the cationic surface results in a surface which is less insulating and possibly less structured. The capacitance values of the underlying HEX and TMA SAM were 2.16–2.63 and 4.66–4.94 μF/cm^2, respectively.

Characterization by AFM. The HFBI layers were imaged using AFM to see if there are differences in morphology between the protein layers on HEX and TMA surfaces. The layers on both substrates had a very similar appearance and were covering the substrate evenly without observable defects. Specific features on the molecular scale could not be identified. The rms roughness (standard deviation of the height values) of the protein layers on TMA and HEX was 2.2 and 1.2 nm, respectively.

4. DISCUSSION

In this work we have shown that class II hydrophobins can bind to polar surfaces that are immersed in aqueous solution under controlled pH and salinity. Hydrophobins did bind to cationic, but not anionic, surfaces and resulted in a significant decrease in polarity of the surface, measured as an increase in water contact angle (WCA). The binding was highly dependent on pH with the largest increase in WCA occurring between pH 8 and 9. At these pH values the hydrophobin layer had a mass corresponding to a monomolecular layer of protein. The binding and resulting WCA values were highly dependent on the ionic strength of the solution, which together with the strong pH dependency indicates that electrostatic forces were important for the interaction between the hydrophobin and the polar surface.

The WCAs of hydrophobin layers on the cationic surfaces were at their highest about 70° (Figure 4B). In control experiments surfaces were treated with the same solutions but not containing protein which resulted in WCAs of about 30°. Thus the presence of hydrophobin gave an approximate 40°

dx.doi.org/10.1021/la300501u | Langmuir 2012, 28, 4293–4300

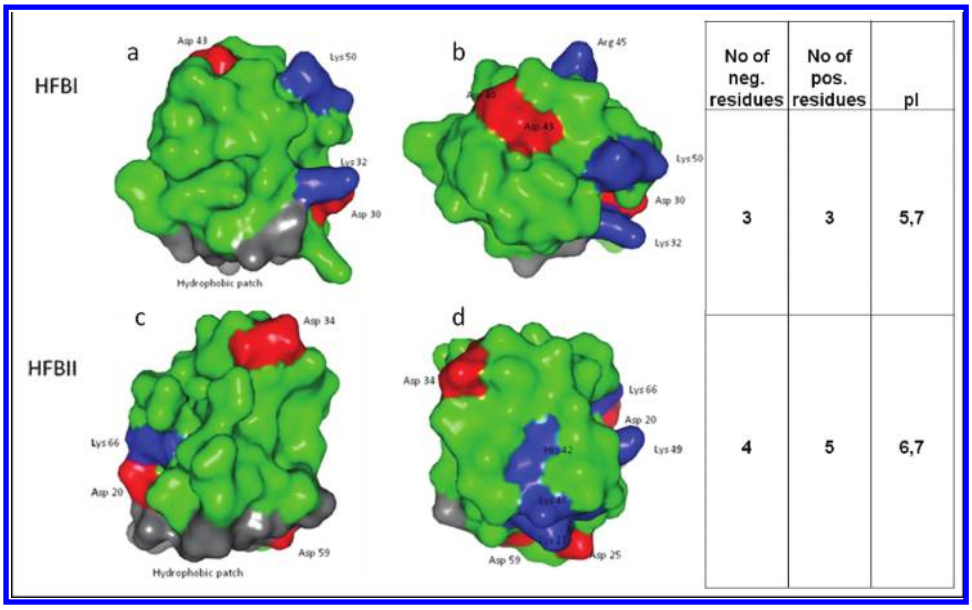

	No of neg. residues	No of pos. residues	pI
HFBI	3	3	5,7
HFBII	4	5	6,7

Figure 8. Structure of HFBI and HFBII. Part a or c shows the protein with the hydrophobic patch (gray) at the bottom, and part b or d show a top view of a or c. The ionizable side chains are shown where red is negative and blue is positive charge in neutral pH. The number of charged residues and pI of the proteins are also shown.

increase in WCA. The behavior is in clear contrast to the binding of hydrophobin to hydrophobic surfaces (Figure 3), where the hydrophobin layer resulted in a drop of contact angle from slightly over 90° to 40−50°, i.e. a decrease of 40−50°. Our interpretation of these data is that the layers that the hydrophobins form are amphiphilic with one side giving a low contact angle and the other giving a higher contact angle. On the hydrophobic surface, the hydrophilic side of the layer is turned toward the solution and on the cationic surface the more hydrophobic side of the layer is turned toward the solution. Previous reports support this view as it has been shown that hydrophobins form layers that have a thickness corresponding to a monomolecular layer on surfaces and interfaces.[14,27] Previously it was also shown that these layers are oriented so that the hydrophilic part of the protein is turned toward the aqueous side at the air−water interface.[14]

We suggest that the process for forming layers with higher contact angles has a biological significance since it could form a part of a mechanism by which hydrophobins participate in the formation of hydrophobic structures in fungi such as mycelium or spores. However, the WCA of the membranes formed in our experiments were still significantly more polar than measured for fungal mycelia (approximately 140°; Figure 1). There are several possible causes for this difference. On the surface of mycelia, it is expected that structural arrangements with other cell wall components as well as geometrical effects such as curvature can play an essential role for its surface properties. The formation of the hydrophobicity of mycelium may also require the participation of additional components. We can also expect that the formation of cell wall structures during fungal growth is a concerted event involving several components.

Nonetheless, it is noteworthy that in the procedure used here the hydrophobin must overcome a substantial energy barrier in order to increase the WCA by assembly in a fully submerged aqueous environment. The driving force for this energetically unfavorable process must be coupled to the self-assembly process that forms surface layers of hydrophobin. In comparison the self-assembly process should then be more favorable. An indication for the mechanism involved came from the observation in experiments on cationic surfaces that the initial amount of protein was initially large and then decreased during extensive washing. As seen in Figure 2, the initial binding on TMA was almost twice of that amount which is left after rinsing. In comparison, the corresponding initial amount bound on HEX or MUA was much smaller. The behavior on TMA could be explained by initial binding as a double layer with a subsequent removal of the outer layer, leaving only the single adsorbed layer after washing. Therefore, a high contact angle surface would not necessarily be formed while exposed to water but could initially form as the base part of a bilayer and being exposed only after the outer layer has been washed off.

To get a deepened understanding of the structure of the adsorbed membranes, they were analyzed by impedance spectroscopy, QCM, and AFM. The QCM and AFM did not reveal any differences when hydrophobin on cationic TMA SAM surface was compared to the corresponding layers on hydrophobic HEX SAM surface. In QCM the dissipation value indicated a rigid layer in both cases and the change in resonance frequency indicated a similar mass. Comparing AFM images of the two layers showed smooth surfaces in both cases but with the hydrophobin−TMA surface having a slightly higher roughness. The images did not show molecular details as previously have been obtained for layers on atomically smooth surfaces such as mica and graphite.[13,14] The reason for this is that the relative roughness of underlying gold case posed limitations for the image resolution. The data obtained by impedance spectroscopy indicated that the hydrophobin layers on the cationic surface were less insulating than the layers formed on hydrophobic surfaces. An interpretation of these data is that the hydrophobin on the cationic surfaces in some manner contains more defects or irregularities. As such irregularities were not identified by AFM, they probably occur more on the molecular or nanoscale and are structurally not easily characterized.

To verify the role of cationic charge on surfaces, we conducted experiments to compare the TMA SAM and a

dx.doi.org/10.1021/la300501u | Langmuir 2012, 28, 4293−4300

structurally very different spin coated PEI polymer surface (Figure 5). Experiments using either surface showed very similar results, although the final WCAs on PEI were slightly lower (Figure 5). These results indicate that the charge of the surface is more important than the structural composition of the underlying surface. However, charge was very important as noted by the completely different results obtained on anionic surfaces (Figure 6) which resulted in very low binding and low differences in WCA.

The molecular details of how the hydrophobins interact with polar surfaces are still unknown. We note however that the hydrophilic side of both HFBI and HFBII show ionizable side chains.[4,5] HFBI has three positively and three negatively charged groups while HFBII has five positively and four negatively changed groups, and their pI values are 5.7 and 6.7 respectively (Figure 8). The lowest binding of both proteins occurred at their respective pI values, although it should be noted that pI represents an average for the whole protein while electrostatic interactions may affect more local environments. The structure of HFBIII is currently unknown but a homology model of HFBIII structure (data not shown) shows that HFBIII has four positively and five negatively charged groups on its hydrophilic side.

In the literature, there are reports describing the difference in polarity of the different sides of layers of class I hydrophobins.[10,20,21,35−37] In these studies, a very different route for forming layers was used. First, membranes were allowed to form at the air−water interface. Then they were deposited on a support typically by drying on polar surfaces such as filter paper. These studies show that hydrophobic membranes can efficiently be formed in this way and the resulting membranes have had high contact angles, sometimes up to 120° (class I hydrophobins). However, preorganization at the air−water interface is unlikely the explanation for how hydrophobins assemble in fungal structures, for example on spores.

Previously Martin et al.[28,38] showed that the class I hydrophobin SC3 could assemble on hydrophilic mica in solution, but this required the presence of the polysaccharide schizophyllan. Both SC3 and schizophyllan are produced by the same organism, *Schizophyllum commune*. In the presence of schizophyllan, the protein layer became highly insoluble and changed the surface contact angle of mica from about 0° to 20−30°, i.e. a much smaller change than found in this study, suggesting a different type of arrangement. The interactions with schizophyllan led to the suggestion that the polysaccharide has a role in stabilizing and ordering the SC3 protein prior to assembly. The effect of poly- and monosaccharides on hydrophobin assembly has been observed in other studies as well.[39,40]

Although our data in the present study using class II hydrophobins shows different details than Martin et al. found for SC3, both studies emphasize the importance of interactions of the hydrophilic part of the protein with other components. However, in nature the polymer−protein interactions can be much more complex and specific and structural features such as surface curvature can play a large role. Nonetheless we show that polar surfaces can act as supports for the formation of hydrophobin membranes. The formation of molecular membranes on different types of interfaces appears to be central to most of the biological functions of hydrophobins as well as for a number of emerging technical applications. Studying these interactions leads to the possibility to understand the molecular structure of fungal spores, cell walls, or fruiting bodies. Also since hydrophobins have received much attention as industrially useful proteins,[3] the hydrophilic assembly can pave the way for new inventions and applications.

AUTHOR INFORMATION

Corresponding Author

*E-mail: markus.linder@vtt.fi.

Notes

The authors declare no competing financial interest.

ACKNOWLEDGMENTS

Riitta Suihkonen is thanked for technical assistance. Olof Andersson and Julia Hedlund at Layerlab are thanked for help with impedance measurements. Financial support from the Academy of Finland is acknowledged. A researcher visit was supported by COST TD0906 Biological Adhesives.

REFERENCES

(1) Linder, M. B.; Szilvay, G. R.; Nakari-Setala, T.; Penttila, M. E. Hydrophobins: the protein-amphiphiles of filamentous fungi. *FEMS Microbiol Rev* **2005**, *29* (5), 877−96.

(2) Wessels, J. G. H. Developmental Regulation of Fungal Cell-Wall Formation. *Ann. Rev. Phytopathol.* **1994**, *32*, 413−437.

(3) Linder, M. B. Hydrophobins: Proteins that self assemble at interfaces. *Curr. Opin. Colloid Interface Sci.* **2009**, *14* (5), 356−363.

(4) Hakanpaa, J.; Paananen, A.; Askolin, S.; Nakari-Setala, T.; Parkkinen, T.; Penttila, M.; Linder, M. B.; Rouvinen, J. Atomic resolution structure of the HFBII hydrophobin, a self-assembling amphiphile. *J. Biol. Chem.* **2004**, *279* (1), 534−9.

(5) Hakanpaa, J.; Szilvay, G. R.; Kaljunen, H.; Maksimainen, M.; Linder, M.; Rouvinen, J. Two crystal structures of Trichoderma reesei hydrophobin HFBI--the structure of a protein amphiphile with and without detergent interaction. *Protein Sci.* **2006**, *15* (9), 2129−40.

(6) Kwan, A. H.; Winefield, R. D.; Sunde, M.; Matthews, J. M.; Haverkamp, R. G.; Templeton, M. D.; Mackay, J. P. Structural basis for rodlet assembly in fungal hydrophobins. *Proc. Natl. Acad. Sci. USA* **2006**, *103* (10), 3621−6.

(7) Wösten, H. A.; Asgeirsdottir, S. A.; Krook, J. H.; Drenth, J. H.; Wessels, J. G. The fungal hydrophobin Sc3p self-assembles at the surface of aerial hyphae as a protein membrane constituting the hydrophobic rodlet layer. *Eur. J. Cell Biol.* **1994**, *63* (1), 122−9.

(8) Wösten, H. A.; van Wetter, M. A.; Lugones, L. G.; van der Mei, H. C.; Busscher, H. J.; Wessels, J. G. How a fungus escapes the water to grow into the air. *Curr. Biol.* **1999**, *9* (2), 85−8.

(9) Talbot, N. J. Fungal biology. Coming up for air and sporulation. *Nature* **1999**, *398* (6725), 295−6.

(10) Lugones, L. G.; Bosscher, J. S.; Scholtmeyer, K.; de Vries, O. M.; Wessels, J. G. An abundant hydrophobin (ABH1) forms hydrophobic rodlet layers in Agaricus bisporus fruiting bodies. *Microbiology* **1996**, *142* (Pt 5), 1321−9.

(11) Wang, Z.; Lienemann, M.; Qiau, M.; Linder, M. B. Mechanisms of protein adhesion on surface films of hydrophobin. *Langmuir* **2010**, *26* (11), 8491−6.

(12) Cox, A. R.; Cagnol, F.; Russell, A. B.; Izzard, M. J. Surface properties of class ii hydrophobins from Trichoderma reesei and influence on bubble stability. *Langmuir* **2007**, *23* (15), 7995−8002.

(13) Paananen, A.; Vuorimaa, E.; Torkkeli, M.; Penttila, M.; Kauranen, M.; Ikkala, O.; Lemmetyinen, H.; Serimaa, R.; Linder, M. B. Structural hierarchy in molecular films of two class II hydrophobins. *Biochemistry* **2003**, *42* (18), 5253−8.

(14) Szilvay, G. R.; Paananen, A.; Laurikainen, K.; Vuorimaa, E.; Lemmetyinen, H.; Peltonen, J.; Linder, M. B. Self-assembled hydrophobin protein films at the air-water interface: structural analysis and molecular engineering. *Biochemistry* **2007**, *46* (9), 2345−54.

(15) Kisko, K.; Szilvay, G. R.; Vuorimaa, E.; Lemmetyinen, H.; Linder, M. B.; Torkkeli, M.; Serimaa, R. Self-assembled films of

hydrophobin proteins HFBI and HFBII studied in situ at the air/water interface. *Langmuir* **2009**, *25* (3), 1612−9.
(16) Wösten, H. A.; Schuren, F. H.; Wessels, J. G. Interfacial self-assembly of a hydrophobin into an amphipathic protein membrane mediates fungal attachment to hydrophobic surfaces. *EMBO J.* **1994**, *13* (24), 5848−54.
(17) Takahashi, T.; Maeda, H.; Yoneda, S.; Ohtaki, S.; Yamagata, Y.; Hasegawa, F.; Gomi, K.; Nakajima, T.; Abe, K. The fungal hydrophobin RolA recruits polyesterase and laterally moves on hydrophobic surfaces. *Mol. Microbiol.* **2005**, *57* (6), 1780−1796.
(18) Nakari-Setala, T.; Aro, N.; Ilmen, M.; Munoz, G.; Kalkkinen, N.; Penttila, M. Differential expression of the vegetative and spore-bound hydrophobins of Trichoderma reesei--cloning and characterization of the hfb2 gene. *Eur. J. Biochem.* **1997**, *248* (2), 415−23.
(19) Bell-Pedersen, D.; Dunlap, J. C.; Loros, J. J. The Neurospora circadian clock-controlled gene, ccg-2, is allelic to eas and encodes a fungal hydrophobin required for formation of the conidial rodlet layer. *Genes Dev.* **1992**, *6* (12A), 2382−94.
(20) De Vries, O. M.; Moore, S.; Arntz, C.; Wessels, J. G.; Tudzynski, P. Identification and characterization of a tri-partite hydrophobin from Claviceps fusiformis. A novel type of class II hydrophobin. *Eur. J. Biochem.* **1999**, *262* (2), 377−85.
(21) Askolin, S.; Linder, M.; Scholtmeijer, K.; Tenkanen, M.; Penttila, M.; de Vocht, M. L.; Wosten, H. A. Interaction and comparison of a class I hydrophobin from Schizophyllum commune and class II hydrophobins from Trichoderma reesei. *Biomacromolecules* **2006**, *7* (4), 1295−301.
(22) De Stefano, L.; Rea, I.; Giardina, P.; Armenante, A.; Rendina, I. Protein-modified porous silicon nanostructures. *Adv. Mater.* **2008**, *20* (8), 1529−+.
(23) Wang, X.; Shi, F.; Wosten, H. A.; Hektor, H.; Poolman, B.; Robillard, G. T. The SC3 hydrophobin self-assembles into a membrane with distinct mass transfer properties. *Biophys. J.* **2005**, *88* (5), 3434−43.
(24) Houmadi, S.; Ciuchi, F.; De Santo, M. P.; De Stefano, L.; Rea, I.; Giardina, P.; Armenante, A.; Lacaze, E.; Giocondo, M. Langmuir-Blodgett Film of Hydrophobin Protein from Pleurotus ostreatus at the Air-Water Interface. *Langmuir* **2008**, *24* (22), 12953−12957.
(25) Wosten, H.; De Vries, O.; Wessels, J. Interfacial Self-Assembly of a Fungal Hydrophobin into a Hydrophobic Rodlet Layer. *Plant Cell* **1993**, *5* (11), 1567−1574.
(26) Aimanianda, V.; Bayry, J.; Bozza, S.; Kniemeyer, O.; Perruccio, K.; Elluru, S. R.; Clavaud, C.; Paris, S.; Brakhage, A. A.; Kaveri, S. V.; Romani, L.; Latge, J. P. Surface hydrophobin prevents immune recognition of airborne fungal spores. *Nature* **2009**, *460* (7259), 1117−21.
(27) Linder, M.; Szilvay, G. R.; Nakari-Setala, T.; Soderlund, H.; Penttila, M. Surface adhesion of fusion proteins containing the hydrophobins HFBI and HFBII from Trichoderma reesei. *Protein Sci.* **2002**, *11* (9), 2257−66.
(28) Martin, G. G.; Cannon, G. C.; McCormick, C. L. Adsorption of a fungal hydrophobin onto surfaces as mediated by the associated polysaccharide schizophyllan. *Biopolymers* **1999**, *49* (7), 621−633.
(29) Linder, M.; Selber, K.; Nakari-Setala, T.; Qiao, M.; Kula, M. R.; Penttila, M. The hydrophobins HFBI and HFBII from Trichoderma reesei showing efficient interactions with nonionic surfactants in aqueous two-phase systems. *Biomacromolecules* **2001**, *2* (2), 511−7.
(30) Ulman, A. Formation and Structure of Self-Assembled Monolayers. *Chem. Rev.* **1996**, *96* (4), 1533−1554.
(31) Hall, H. K. Correlation of the Base Strengths of Amines. *J. Am. Chem. Soc.* **1957**, *79* (20), 5441−5444.
(32) Sugihara, K.; Teranishi, T.; Shimazu, K.; Uosaki, K. Structure dependence of the surface pKa of mercaptoundecanoic acid SAM on gold. *Electrochemistry* **1999**, *67* (12), 1172−1174.
(33) Rodahl, M.; Hook, F.; Fredriksson, C.; Keller, C. A.; Krozer, A.; Brzezinski, P.; Voinova, M.; Kasemo, B. Simultaneous frequency and dissipation factor QCM measurements of biomolecular adsorption and cell adhesion. *Faraday Discuss* **1997**, *107*, 229−46.
(34) Hedlund, J.; Lundgren, A.; Lundgren, B.; Elwing, H. A new compact electrochemical method for analyzing complex protein films adsorbed on the surface of modified interdigitated gold electrodes. *Sens. Actuators B−Chem.* **2009**, *142* (2), 494−501.
(35) Lugones, L. G.; Wosten, H. A.; Wessels, J. G. A hydrophobin (ABH3) specifically secreted by vegetatively growing hyphae of Agaricus bisporus (common white button mushroom). *Microbiology* **1998**, *144* (Pt 8), 2345−53.
(36) Lugones, L. G.; Scholtmeijer, K.; Klootwijk, R.; Wessels, J. G. Introns are necessary for mRNA accumulation in Schizophyllum commune. *Mol. Microbiol.* **1999**, *32* (4), 681−9.
(37) Scholtmeijer, K.; Janssen, M. I.; Gerssen, B.; de Vocht, M. L.; van Leeuwen, B. M.; van Kooten, T. G.; Wosten, H. A.; Wessels, J. G. Surface modifications created by using engineered hydrophobins. *Appl. Environ. Microbiol.* **2002**, *68* (3), 1367−73.
(38) Martin, G. G.; Cannon, G. C.; McCormick, C. L. Sc3p hydrophobin organization in aqueous media and assembly onto surfaces as mediated by the associated polysaccharide schizophyllan. *Biomacromolecules* **2000**, *1* (1), 49−60.
(39) Armenante, A.; Longobardi, S.; Rea, I.; De Stefano, L.; Giocondo, M.; Silipo, A.; Molinaro, A.; Giardina, P. The Pleurotus ostreatus hydrophobin Vmh2 and its interaction with glucans. *Glycobiology* **2010**, *20* (5), 594−602.
(40) Scholtmeijer, K.; de Vocht, M. L.; Rink, R.; Robillard, G. T.; Wosten, H. A. Assembly of the fungal SC3 hydrophobin into functional amyloid fibrils depends on its concentration and is promoted by cell wall polysaccharides. *J. Biol. Chem.* **2009**, *284* (39), 26309−14.